Polarizing Beam-Splitter Based on Defective Photonic Crystals

S. Roshan Entezar

Faculty of Physics, University of Tabriz, Tabriz, Iran

s-roshan@tabrizuni.ac.ir

ABSTRACT— The performance of a polarizing beam splitter based on the one-dimensional photonic crystals (1D-PCs), is theoretically investigated. The polarizing beam splitter consists of a symmetric stack of the low-index quarter-wave plates and the high-index half-wave plates with a central defect layer of air. The linear transmission properties of the polarizing beam splitter are numerically simulated by the transfer matrix method. The results show that the wavelength of the polarizing beam splitter can be tuned by adjusting the thickness of the defect layer of air and the incident angle of light due to the resonant couple of the evanescent waves localized at the interfaces between neighboring layers.

KEYWORDS: Polarizer, Beam-splitter, Defective photonic crystal, Evanescent waves

I. INTRODUCTION

Photonic crystals (PCs) as structures having materials with periodically modulated dielectric constants in one, two and three-dimensions have been the subjects of intensive studies due to their unique electromagnetic properties and potential applications [1–4]. Under some circumstances, certain ranges of the optical wavelengths (i.e. the photonic band gaps (PBGs)) are forbidden to propagate inside the PC [1]. It is known that one can attain a very narrow defect mode inside the PBG by creating defects in the periodic structure of the PCs [2]. This unique feature of the PC which alters dramatically the flow of light within the structure, can lead to many potential applications in optoelectronics [4, 5]. Since, the 1D-PCs are easier to fabricate, many interesting applications such as dielectric reflecting mirrors, low-loss waveguides, optical switches, filters, and optical limiters have been suggested based on the 1D-PCs [6–11]. It has been demonstrated theoretically and experimentally that the 1D-PCs have absolute omnidirectional PBGs [12–14]. Recently, the application of the 1D-PCs as polarizing beam splitters has attracted a great deal of attention due to their importance in the fields of optical interconnection, ultrafast light information processing and optoelectronic signal receiving or detecting systems [15–18].

In this paper, we study the transmission properties of a 1D-PC composed of alternating layers of high index and low index dielectric materials with a central defect layer of air in it. Unlike the previous studies that the waves are incident form the air to the structure, in the present study we assume that the waves are incident form a dense medium to the structure. In this case, the waves will be evanescent in the low index layers and we have propagating waves in the high index layers at the incident angles greater than a critical angle. Thus some unusual transmissions will be found, and the structure can be used as a tunable multichannel polarizing beam splitter. The polarizing characteristics of the 1D-PC structures are realized by the resonant couple of the evanescent waves localized at the interfaces between neighboring layers. The thickness of the defect layer of air plays an important role to fine tune the wavelength of the polarizing beam splitter. In Section 2, we present the model and the basic theory of the polarizing beam splitter. Section 3 is devoted to the analysis of the system. In Section 4, we present a summary of our main results.

II. THEORY OF POLARIZING BEAM-SPLITTER
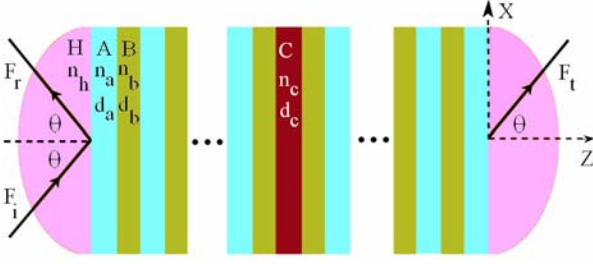
Fig. 1. Schematic representation of the 1D layered structure $H(AB)^m C(BA)^m H$.

Consider the 1D layered structure $H(AB)^m C(BA)^m H$ shown in Fig. 1, where, m is the period number, A and B represent the low index and the high index dielectric layers with the thicknesses d_a, d_b and refractive indices n_a, n_b, respectively. C is a defect layer of air with the refractive index n_c and the thickness d_c. Here, we assumed that the layered structure is surrounded by the medium H with the refractive index n_h.

Let a plane wave with temporal part $\exp(i\omega t)$ be injected from the medium H into the 1D layered structure at the incident angle θ, as shown in Fig. 1. The reflectance and transmittance coefficients of the structure can be calculated by the transfer matrix method (TMM) [19]:

$$R = \frac{\left| M_{21} + \frac{ik_{hz}}{\alpha_h} M_{22} \right|}{\left| M_{11} + \frac{ik_{hz}}{\alpha_h} M_{12} \right|}, T = \frac{1}{\left| M_{11} + \frac{ik_{hz}}{\alpha_h} M_{12} \right|}. \quad (1)$$

where M_{11}, M_{12}, M_{21}, and M_{22} are the elements of total transfer matrix of the system (M) which is given as:

$$M = (M_a M_b)^m M_c (M_b M_a)^m, \quad (2)$$

and

$$M_j = \begin{pmatrix} \cos k_{jz}d_j & -\frac{\alpha_j}{k_{jz}}\sin k_{jz}d_j \\ \frac{k_{jz}}{\alpha_j}\sin k_{jz}d_j & \cos k_{jz}d_j \end{pmatrix}, \quad (3)$$

with $k_{jz} = \frac{\omega}{c}\sqrt{n_j^2 - n_h^2 \sin^2\theta}$ (j = a, b, c) and

$$\alpha_j = \begin{cases} 1 & for & \text{TE polarization} \\ n_j^2 & for & \text{TM polarization} \end{cases}. \quad (4)$$

III. RESULTS AND DISCUSSION

In what follow we assume that the layered structure is constructed from the quarter-wave plates A and the half-wave plates B. The used materials are chosen to be polydiacetylene 9-BCMU with the refractive index $n_a = 1.55$ and Si with the refractive index $n_b = 3.48$ [20, 21]. We consider the thicknesses of the layers as $2n_a d_a = n_b d_b = 275\,nm$, $n_c = 1$ and $n_h = n_b$. We want to discuss the effect of the defect layer of air on the performance of the polarizing beam splitter. To do this, we first plot the transmission spectra of the 1D defective multilayer structure $H(AB)^4 C(BA)^4 H$ as a function of vacuum wavelength (λ) for the TE-polarized (the solid lines) and the TM-polarized (the dashed lines) waves at the incident angles a) $\theta = 0°$, b) $\theta = 20°$, c) $\theta = 30°$ with $d_c = 0$ and d) $\theta = 0°$, e) $\theta = 20°$, f) $\theta = 30°$ with $d_c = d_a$ in Fig. 2. As it is clear from the figure, the structure contains a wide transmission band in the visible range at the normal incidence case (see Fig. 2(a)). However, by increasing the incident angle θ, the structure shows a wide band gap with some resonant transmission lines (see the case $\theta = 30°$ in Fig. 2). Moreover, the vacuum wavelength of the resonant transmission lines depending on the polarization of the incident waves can be fine tuned by adjusting the width of the defect layer of air (see Figs. 2(d,e,f)). These resonant transmission lines are due to the interaction of the evanescent waves in the low-index layers and the propagating waves in the high-index layers.
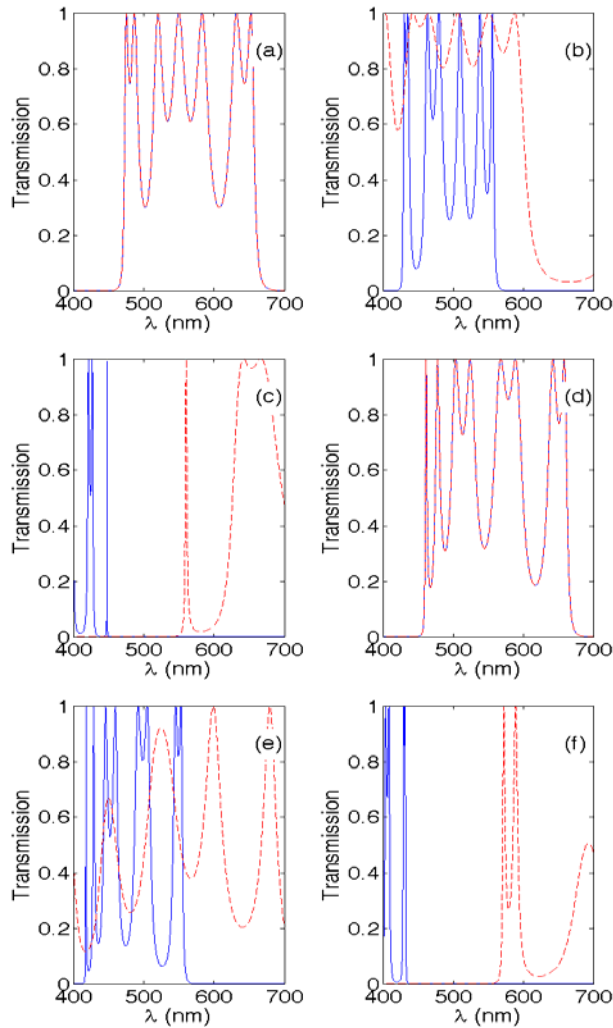
Fig. 2. Transmission spectra of the layered structure $H(AB)^4C(BA)^4H$ as a function of vacuum wavelength (λ) for the TE-polarized (the solid lines) and the TM-polarized (the dashed lines) waves at the incident angles a) $\theta = 0°$, b) $\theta = 20°$, c) $\theta = 30°$ with $d_c = 0$ and d) $\theta = 0°$, e) $\theta = 20°$, f) $\theta = 30°$ with $d_c = d_a$ Here, we assumed that $n_a = 1.55$, $n_b = 3.48$, $n_c = 1$, $n_h = n_b$ and $2n_a d_a = n_b d_b = 225\,nm$.

For our choice of the parameters, the waves are evanescent in the layers *A* for $\theta > \sin^{-1} n_a / n_h = 26.5°$. Furthermore, for $\theta > \sin^{-1} n_c / n_h = 16.7°$ the waves are evanescent in the defect layer *C*. As one can see from the Fig. 2, for one of the polarizations the transmittance of the structure reaches to 100% at the resonant wavelengths. While, for the other polarization the transmittance of the structure reaches nearly to zero (see Figs. 2(c,f)). So, one of the polarizations at the

resonant wavelength completely transmitted from the structure and the other one completely reflected from the structure. As a result, the structure acts as a polarizing beam splitter. To show more clearly the angular behavior of the resonant transmission lines, we plotted the transmission of the structure $H(AB)^4C(BA)^4H$ on the plane of λ and θ for a) the TE-polarized wave, b) the TM-polarized wave with $d_c = 0$ and c) the TE-polarized wave, d) the TM-polarized wave with $d_c = d_a$ in Fig. 3.
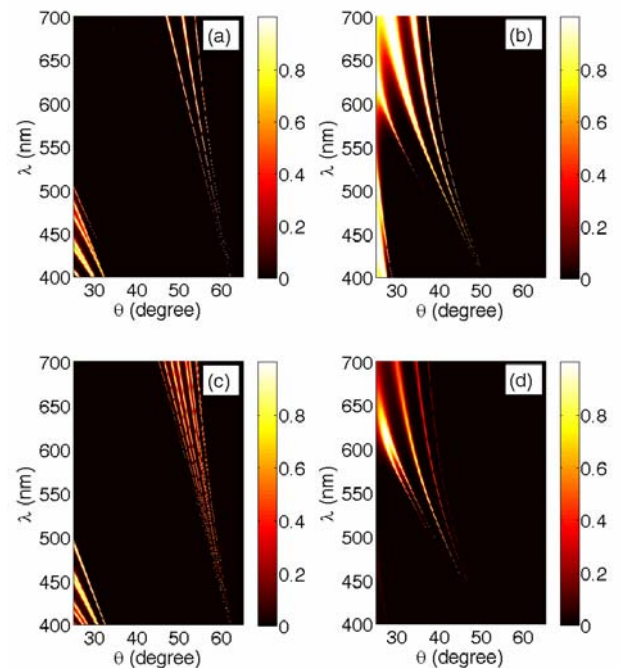
Fig. 3. Transmission of the structure $H(AB)^4C(BA)^4H$ on the plane of wavelength and incident angle for a) the TE-polarized wave, b) the TM-polarized wave with $d_c = 0$ and c) the TE-polarized wave, d) the TM-polarized wave with $d_c = d_a$. Other parameters are the same as those of Fig. 2.

Here, the light regions show the transmission peaks and the dark regions show the forbidden band gaps. This figure reveals that the wavelengths of the resonant transmission peaks not only depend on the polarization of the incident wave, but also on the width of the defect layer of air which can be easily adjusted. Additionally, the number of the

resonant transmission peaks depends on the width of the defect layer of air.

Now, we want to show that the working wavelength of the system can be tuned simply by adjusting the width of the defect layer of air. To show this, the transmission of the structure $H(AB)^4C(BA)^4H$ is plotted versus d_c/d_a for the TE-polarized (the solid lines) and the TM-polarized (the dashed lines) waves at the vacuum wavelengths a) $\lambda = 431\,nm$ and b) $\lambda = 572\,nm$ with $\theta = 30°$ in Fig. 4.
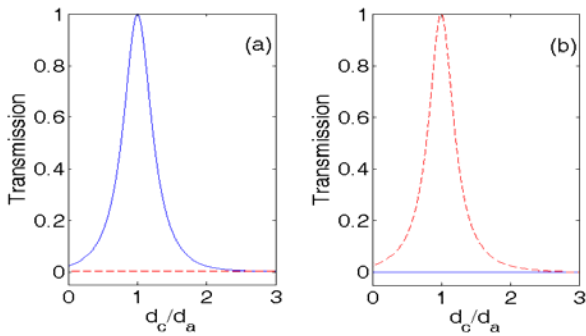
Fig. **4.** Transmission of the structure $H(AB)^4C(BA)^4H$ versus d_c/d_a for the TE-polarized (the solid lines) and the TM-polarized (the dashed lines) waves at the vacuum wavelengths a) $\lambda = 431\,nm$ and b) $\lambda = 572\,nm$. Here, we assumed that $\theta = 30°$ and the other parameters are the same as those of Fig. 2.

Figure 4(a) shows that the transmittance of the TE-polarized waves at $\lambda = 431\,nm$ increases by increasing d_c and reaches to its maximum value 100% at $d_c = d_a$ and then it is decreases by further increasing d_c. However, the transmittance of the TM-polarized wave at $\lambda = 431\,nm$ independent from the value of d_c is nearly zero (see dashed lines in Fig. 4(a)). This situation is vice versa at $\lambda = 572\,nm$ (see Fig. 4(b)). So, the working wavelength of the polarizing beam splitter can be tuned by adjusting the width of the air layer. To display more clearly the effect of the defect layer of air on the operating wavelength of the polarizing beam splitter, we plotted the transmission spectra of the structure $H(AB)^4C(BA)^4H$ on the plane of λ and

d_c/d_a for a) the TE-polarized wave and b) the TM-polarized wave at the incident angle $\theta = 30°$ in Fig. 5. The figure clearly shows that the operating wavelength of the polarizing beam splitter can be tuned simply by adjusting the thickness of the defect layer of air at the given incident angle.
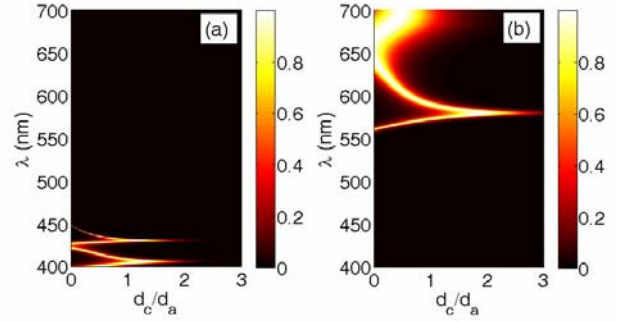
Fig. **5.** Transmission of the structure $H(AB)^4C(BA)^4H$ on the plane of wavelength and d_c/d_a for a) the TE-polarized wave, b) the TM-polarized wave at the incident angle $\theta = 30°$. Other parameters are the same as those of Fig. 2.
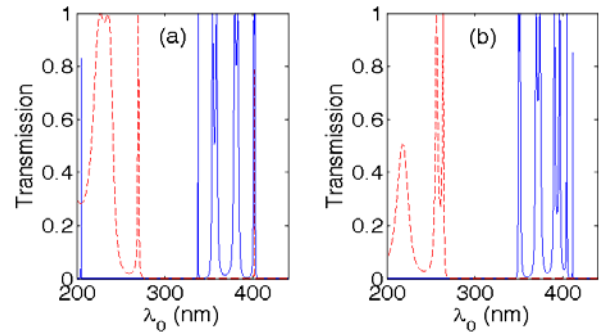
Fig. **6.** Transmission of the structure $H(AB)^4C(BA)^4H$ versus λ_0 for the TE-polarized and the TM-polarized waves at the vacuum wavelength $\lambda = 550\,nm$ with a) $d_c = 0$ and b) $d_c = d_a$. Here, $\theta = 30°$, the optical thicknesses of the layers A and B are given by $2n_a d_a = n_b d_b = \lambda_0$ and the other parameters are the same as those of Fig. 2.

In continue, we consider the effect of the optical thicknesses of the layers A and B on the transmission of the structure at the given wavelength λ. Here, we assume that the optical thicknesses of the layers A and B are given by $2n_a d_a = n_b d_b = \lambda_0$. Figure 6 shows the transmission of the structure $H(AB)^4C(BA)^4H$ versus λ_0 for the TE-polarized and the TM-

polarized waves at the vacuum wavelength $\lambda = 550\,nm$ and the incident angle $\theta = 30°$ with a) $d_c = 0$ and b) $d_c = d_a$. This figure reveals that the optical thicknesses of the layers A and B play essential role in designing a polarizing beam splitter for a given operating wavelength. Moreover, one can use the width of the defect layer of air as a controlling parameter to adjust the working wavelength of the polarizing beam splitter (see Fig. 6(c, d)).
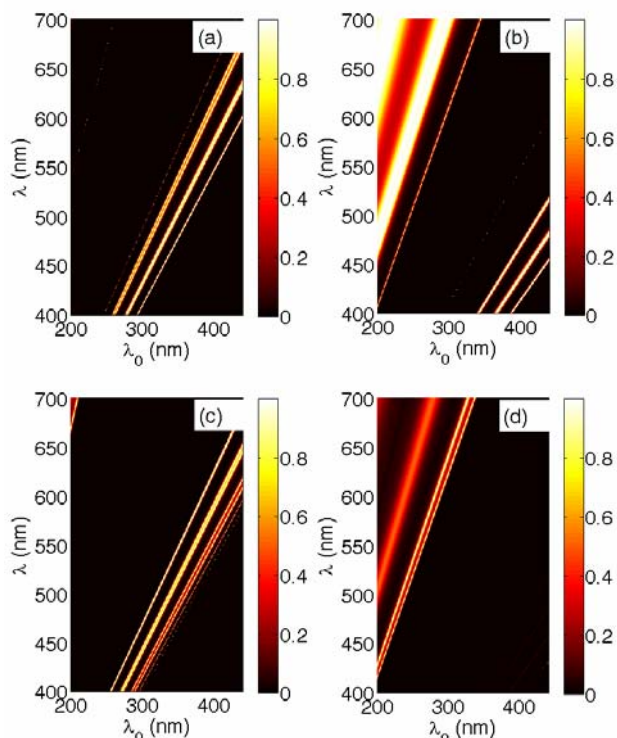
Fig. 7 Transmission of the structure $H(AB)^4 C(BA)^4 H$ on the plane of wavelentgh and λ_0 for a) the TE-polarized, b) the TM-polarized waves with $d_c = 0$ and c) TE polarization, d) TM polarization with $d_c = d_a$. Here, the incident angle is $\theta = 30°$, the optical thicknesses of layers A and B are given by $2n_a d_a = n_b d_b = \lambda_0$ and the other parameters are same as Fig. 2.

In order to show the role of the optical thicknesses of the constituting layers of the structure on the performance of the polarizing beam splitter at the visible range, we plotted the transmission spectra of the structure $H(AB)^4 C(BA)^4 H$ on the plane of λ and λ_0 for a) the TE-polarized wave, b) the TM-

polarized wave with $d_c = 0$ and c) the TE-polarized wave, d) the TM-polarized wave with $d_c = d_a$ in Fig. 7. Here, we considered again $2n_a d_a = n_b d_b = \lambda_0$ and $\theta = 30°$. Form Fig. 7 it is clear that the operating wavelength of the polarizing beam splitter depends on the thicknesses of the quarter-wave plates A, the half-wave plates B and the defect layer of air C.

The creation of the resonant transmission peaks in the transmission spectra of the structure is due to the localization of the electromagnetic fields at the interface of the low-index and the high-index layers. To show this, we plotted the normalized transverse electric field intensity distributions in the structure $H(AB)^4 C(BA)^4 H$ for the TE-polarized (the solid lines) and the TM-polarized (the dashed lines) waves at $\lambda = 430\,nm$ with $\theta = 30°$ and $d_c = d_a$ in Fig. 8.
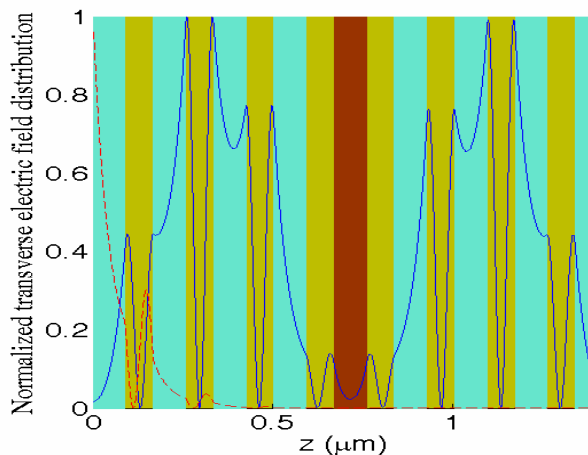
Fig. 8 Normalized transverse electric field intensity distributions in the structure $H(AB)^4 C(BA)^4 H$ for the TE polarized (the solid line) and the TM-polarized (the dashed line) waves at the wavelength of $\lambda = 430\,nm$. Here, $d_c = d_a$, the incident angle is $\theta = 30°$ and the other parameters are same as Fig. 2.

From the Fig. 8, we see that the transverse electric field intensity of the TE-polarized wave has a symmetric distribution around the defect layer of air. Moreover, the transverse electric field intensity of the TE polarized wave is localized at the interface of the low-

index and the high-index layers. Since, the used structure is also symmetric; this means that the structure completely transmits the TE-polarized wave at the given wavelength and incident angle. On the other hand, Fig. 8 shows that the transmission of the structure for the TM-polarized wave is approximately zero. Accordingly, the structure completely reflects the TM-polarized wave.

IV. CONCLUSION

In conclusion, we demonstrated the realization of a polarizing beam splitter in the centro-symmetric one dimensional photonic crystal structure consisting dielectric materials. For the incident angles greater than the critical angle, the electromagnetic waves in the low-index materials are evanescent waves. The thickness of the middle defect layer of air plays an important role for the fine tune of the operating wavelength of the structure. It is shown that different wavelengths can be achieved by adjusting the incident angle and the width of defect layer of air.

REFERENCES

[1]   E. Yablonovitch, "Inhibited Spontaneous Emission in Solid-State Physics and Electronics," Phys. Rev. Lett. Vol. 58 pp. 2059-2062, 1987.

[2]   S. John, "Strong localization of photons in certain disordered dielectric superlattices," Phys. Rev. Lett. Vol. 58, pp. 2486-2489, 1987.

[3]   K. Sakoda, Optical Properties of Photonic Crystals, Springer, Berlin, 2001.

[4]   J.D. Joannopoulos, R.D. Meade, and J.N. Winn, Photonic Crystals: Molding the Flow of Light, Princeton University Press, 1995.

[5]   J.D. Joannopoulos, P.R. Villeneuve, and F. Fan, "Photonic crystals: Putting a new twist on light," Nature, Vol. 386, pp. 143-149, 1997.

[6]   P. Han and H. Wang, "Extension of omnidirectional reflection range in one-dimensional photonic crystals with a staggered structure," J. Opt. Soc. Am. B, Vol. 20, pp. 1996-2001, 2003.

[7]   B.Y. Soon, J.W. Haus, M. Scalora, and C. Sibilia, "One-dimensional photonic crystal optical limiter," Opt. Express, Vol. 11, pp. 2007-2018, 2003.

[8]   K. Yuan, X. Zheng, C.-L. Li, and W.L. She, "Design of omnidirectional and multiple channeled filters using one dimensional photonic crystals containing a defect layer with a negative refractive index," Phys. Rev. E, Vol. 71, pp. 1-5, 2005.

[9]   G. Ma, J. Shen, Z. Zhang , Z. Hua, and S.H. Tang, "Ultrafast all-optical switching in one-dimensional photonic crystal with two defects," Opt. Express, Vol. 14, pp. 858-865, 2006.

[10]   X.H. Zou, W. Pan, B. Luo, W.L. Zhang, and M.Y. Wang, "One-Dimensional Photonic Crystal-Based Multichannel Filters Using Binary Phase-Only Sampling Approach," IEEE J. Lightwave Technology, Vol. 25, pp. 2482-2486, 2007.

[11]   S.H. Xu, X.M. Ding, and Z.Q. Zhu, "TE and TM defective bands splitting in one-dimensional coupled cavity waveguides," Opt. Commun. Vol. 269, pp. 304–309, 2007.

[12]   M. Ibanescu, M.Y. Fink, S. Fan, E.L. Thomas, and J.D. Joannopoulos, "An all-dielectric coaxial waveguide," Science Vol. 289, pp. 415-419, 2000.

[13]   D. Lusk, I. Abdulhalim, and F. Placido, "Omnidirectional reflection from Fibonacci quasi-periodic one-dimensional photonic crystal," Opt. Commun. Vol. 198, pp. 273-279, 2001.

[14]   R. Srivastava, S. Pati, and S.P. Ojha, "Enhancement of omnidirectional reflection in photonic crystal heterostructures," Prog. Electromagn. Res. B, Vol. 1, pp. 197-208, 2008.

[15]   R.M.A. Azzam and H.K. Khanfar, "Broad band IR polarizing beam splitter using a subwavelength-structured one-dimensional photonic-crystal layer embedded in a high-index prism," Appl. Opt. Vol. 48, pp. 5121-5126, 2009.

[16]   K. Yang, X. Long, Y. Huang, and S. Wu, "Design and fabrication of ultra-high precision thin-film polarizing beam splitter," Opt. Commun. Vol. 284, pp. 4650–4653, 2011.

[17] J. Ma and Y. Fan, "Broad band polarizing beam splitter with a dielectric layer embedded in the groove of metal grating," Optics & Laser Technology, Vol. 44, pp. 608–610, 2012.

[18] W. Wanga and X. Rong, "Design of terahertz wave polarizing beam splitter," Optik, Vol. 124, pp. 6089– 6092, 2013.

[19] P. Yeh, Optical Waves in Layered Media, John Wiley & Sons, New York, 1988.

[20] V. Grigoriev and F. Biancalana "Bistability, multistability and non-reciprocal light propagation in Thue–Morse multilayered structures," New J. Phys. Vol. 12, pp. 053041, 2010.

[21] W. Bogaerts, D. Taillaert, B. Luyssaert, P. Bienstman, and R. Baets, "Fabrication of Photonic Crystals in Silicon-on-Insulator Using 248-nm Deep UV Lithography," IEEE J. Sel. Top Quantum Electron. Vol. 8, pp. 928–934, 2002.

Samad Roshan Entezar was born in Tabriz, Iran, in 1969. He received the M.S. degree in physics (atomic and molecular) and the Ph.D. degree in laser physics from university of Tabriz, Iran, in 2001 and 2006, respectively. In 2007, he joined the Physics Department of University of Tabriz as an assistant professor of Physics. His current research activities are in the fields of quantum optics in photonic crystals, linear and nonlinear optics in photonic crystal and metamaterial. Dr. Roshan Entezar has authored and co-authored more than 38 scientific papers in peer-referred international journals.

THIS PAGE IS INTENTIONALLY LEFT BLANK.